Journal of Zhejiang University SCIENCE A
ISSN 1673-565X (Print); ISSN 1862-1775 (Online)
www.zju.edu.cn/jzus; www.springerlink.com
E-mail: jzus@zju.edu.cn

Motion and orientation of cylindrical and cubic particles in pipe flow with high concentration and high particle to pipe size ratio*

Xiao-ke KU[1], Jian-zhong LIN[†‡1,2]

([1]*Department of Mechanics*, *Zhejiang University*, *Hangzhou 310027*, *China*)

([2]*College of Metrology Technology and Engineering, China Jiliang University*, *Hangzhou 310018*, *China*)

[†]E-mail: mecjzlin@public.zju.edu.cn

Received Aug. 30, 2007; revision accepted Dec. 11, 2007; published online Feb. 23, 2008

Abstract: Lattice Boltzmann method was used to numerically investigate the motion and orientation distribution of cylindrical and cubic particles in pipe flow with high concentration and high particle to pipe size ratio. The transient impulse model of 3D collisions between particles and between particle and wall is proposed. The numerical results are qualitatively in agreement with and quantitatively comparable to the experiment data. The results show that the increases of both the cylindrical particle to pipe size ratio and the particle aspect ratio decrease the rotation about all axes. All rotations of cubic particles decrease with increasing the particle concentration. The cubic particles, rotating more drastically in the flow with large Reynolds number, rotate faster than the cylindrical particles with the same size. The cylindrical particles align with the flow direction more obviously with decreasing Reynolds numbers. However, the orientations of cubic particles are spread all over the range with no significant difference in magnitude, and the Reynolds numbers have no obvious effect on the orientations of cubic particles.

Key words: Particulate flow, Angular velocity, Orientation, Lattice Boltzmann method
doi:10.1631/jzus.A071463 **Document code:** A **CLC number:** O359

INTRODUCTION

The investigation of particle transport processes has attracted considerable attention due to their numerous industrial and practical applications. The currently available works on particle transport are exclusively concerned with idealized spherical particles, however, most industrial solid particles are nonspherical. The motions of nonspherical particles in flows are much complicated because the orientation and the rotational motion are strongly coupled with the translation motion.

Cylindrical and cubic particles are one class of nonspherical particles, whose orientation distribution has been a subject of extensive investigation. The motions of cylindrical particles in pipe flows can be found in many areas of industry, such as the production of composite materials, environmental engineering, chemical engineering, textile industry, paper making, and so on. The properties of particles have significant effects on the quality of products. There are some studies devoted to the motions of cylindrical particles. Bernstein and Shapiro (1994) and Lin *et al.*(2002) studied, experimentally and numerically respectively, the orientation distribution of cylindrical particles immersed in a laminar pipe flow. Ding and Aidun (2000) studied the effect of inertia on the dynamics of a solid particle (a circular cylinder, an elliptical cylinder and an ellipsoid) suspended in shear flow. Qi (2001) simulated the fluidization of cylindrical multiparticles in a 3D space. Lin *et al.*(2004) computed the spatial and orientational distributions of cylindrical particles in turbulent pipe flows. Yasuda *et al.*(2005) measured the flow-induced fiber orientation and concentration distributions in channel flows of fiber suspension. Ausias *et al.*(2006) numerically

‡ Corresponding author
* Project (No. 10632070) supported by the National Natural Science Foundation of China

simulated fiber suspensions in transient and steady state shear flows for concentrated solutions. However, most literature has considered the transport of relatively fine particles in the flow. Recent industry interest in sterilization of biomaterials has given new challenges for simulation of particle motion. In the case of sterilization of biomaterials, flows involve two phases where solids-to-pipe diameter ratios are in the range of 0.1~0.3; solids density is typically close to that of the fluid phase. Zitoun *et al.*(2001) adapted the PTV (Particle Tracking Velocimetry) technique to solid-liquid mixtures of high solid concentration and high solid to tube size ratio (up to 1:2) to measure the interstitial velocities in upward flow through a vertical tube. They characterized the rotational velocities of solid objects in these flows and determined the solids orientation angle distribution relating to the flow direction. However, the physical mechanisms responsible for such systems are still not well understood and are subject to debate. Therefore, this study is aimed to use the Lattice Boltzmann method to numerically simulate the motions of cylindrical and cubic particles in pipe flows with high solid concentration and high solid to pipe size ratio, and determine the rotational velocities and orientation distributions of particles.

NUMERICAL METHODS

Unlike the traditional computational schemes based on the continuum assumption of fluids, the original Lattice Boltzmann equation (LBE) in the discrete microscopic velocity space is given as

$$\partial f_i / \partial t + \boldsymbol{e}_i \cdot \nabla f_i = \Omega_i, \tag{1}$$

where f_i is the density distribution function, $\boldsymbol{e}_i$ is the streaming velocity in the ith direction in the phase space, i=1, 2, ..., N, and Ω_i is the collision operator and the BGK collision term given as (Bhatnagar *et al.*, 1954)

$$\Omega_i = -(f_i - f_i^{\mathrm{eq}}) / \tau, \tag{2}$$

where f_i^{eq} is the local equilibrium distribution, τ is the single relaxation time, and for the square or cubic lattice, the equilibrium function f_i^{eq} is taken as (Chen *et al*., 1992):

$$f_i^{\mathrm{eq}} = \rho w_i[1 + 3(\boldsymbol{e}_i \cdot \boldsymbol{u}) / c^2 + 9(\boldsymbol{e}_i \cdot \boldsymbol{u})^2 / (2c^4) - 3u^2 / (2c^2)], \quad i = 0, \cdots, n, \tag{3}$$

where w_i is the weight, $c=\Delta x/\Delta t$ is the lattice speed, ρ and $\boldsymbol{u}$ are the macroscopic fluid density and velocity, respectively,

$$\rho = \sum_i f_i, \ \boldsymbol{u} = \frac{1}{\rho}\sum_i f_i \boldsymbol{e}_i. \tag{4}$$

In the limit of long wavelengths, the LBE recovers the following quasi-incompressible NSEs by the Chapman-Enskog multi-scaling expansion (Chen and Doolen, 1998),

$$\partial \rho / \partial t + \nabla \cdot \rho \boldsymbol{u} = 0, \tag{5}$$

$$\partial \rho \boldsymbol{u} / \partial t + \nabla \cdot \rho \boldsymbol{u}\boldsymbol{u} = -\nabla P + \mu \Delta \boldsymbol{u}, \tag{6}$$

where $P = \rho c_{\mathrm{s}}^2$ is the fluid pressure, c_{s} is the sound speed with $c_{\mathrm{s}}^2 = c^2/3$; $\mu = \rho\nu$ is the dynamic viscosity and $\nu = c^2 \Delta t(\tau - 0.5)/3$.

In this paper, a 3D and 15-bits model as shown in Fig.1 is adopted. The 15 different velocities are listed in Table 1 and the values of the corresponding weights are:

$$w_0 = 2/9; \ w_i = 1/9, \ i = 1 \sim 6; \ w_i = 1/72, \ i = 7 \sim 14. \tag{7}$$

Ladd (1994a; 1994b) used the momentum exchange method to propose a modified bounce-back rule which is for a moving wall. We place the

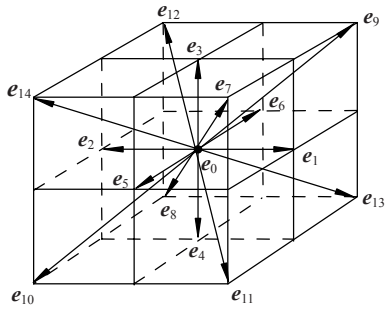

Fig.1 3D and 15-bits model

Table 1 List of 15 velocities

i	$\boldsymbol{e}_i$	i	$\boldsymbol{e}_i$
0	(0,0,0)	8	(−1,−1,−1)
1	(1,0,0)	9	(−1,1,1)
2	(−1,0,0)	10	(1,−1,−1)
3	(0,1,0)	11	(−1,−1,1)
4	(0,−1,0)	12	(1,1,−1)
5	(0,0,1)	13	(1,−1,1)
6	(0,0,−1)	14	(−1,1,−1)
7	(1,1,1)		

boundary nodes on the links connecting the interior and exterior nodes, and obtain:

$$f_{i'}(\boldsymbol{x},t+1)=f_i(\boldsymbol{x},t_+)-2B_i(\boldsymbol{e}_i\cdot\boldsymbol{u}_\mathrm{b}), \tag{8}$$

where "t_+" denotes the post-collision time, i is the incident direction, i' is the reflected direction, $B_i=3\rho w_i/c^2$, $\boldsymbol{u}_\mathrm{b}$ is the velocity on the particle surface. $\boldsymbol{u}_\mathrm{b}=\boldsymbol{u}_0+\boldsymbol{\Omega}\times\boldsymbol{x}_\mathrm{b}$, where $\boldsymbol{u}_0$ is the translational velocity of the mass center of the particle, $\boldsymbol{\Omega}$ is the angular velocity of the particle, and $\boldsymbol{x}_\mathrm{b}=\boldsymbol{x}+\boldsymbol{e}_i/2-\boldsymbol{x}_0$, here $\boldsymbol{x}_0$ is the position of the mass center. The force and torque exerted by the fluid at $\boldsymbol{x}_\mathrm{b}$ are

$$\boldsymbol{F}(\boldsymbol{x}+\boldsymbol{e}_i/2,t)=2\boldsymbol{e}_i[f_i(\boldsymbol{x},t_+)-B_i(\boldsymbol{e}_i\cdot\boldsymbol{u}_\mathrm{b})], \tag{9}$$

$$\boldsymbol{T}(\boldsymbol{x}+\boldsymbol{e}_i/2,t)=\boldsymbol{x}_\mathrm{b}\times\boldsymbol{F}. \tag{10}$$

So the total force and torque on the particle are:

$$\boldsymbol{F}=\sum\boldsymbol{F}(\boldsymbol{x}+\boldsymbol{e}_i/2,t), \tag{11}$$

$$\boldsymbol{T}=\sum\boldsymbol{T}(\boldsymbol{x}+\boldsymbol{e}_i/2,t). \tag{12}$$

Then update the particle velocity and angular velocity according to Newtonian's law.

The particle moves and rotates in 3D space. In the body coordinates of the particle, the 3D rotation is described by Euler equations

$$\dot{\Omega}_x=T_x/I_{xx}+(I_{yy}-I_{zz})\Omega_y\Omega_z/I_{xx}, \tag{13a}$$

$$\dot{\Omega}_y=T_y/I_{yy}+(I_{zz}-I_{xx})\Omega_z\Omega_x/I_{yy}, \tag{13b}$$

$$\dot{\Omega}_z=T_z/I_{zz}+(I_{xx}-I_{yy})\Omega_x\Omega_y/I_{zz}, \tag{13c}$$

where Ω_x, Ω_y, Ω_z are the components of the angular velocity, T_x, T_y, T_z are the torques, I_{xx}, I_{yy}, I_{zz} are the primary inertia moments of the particle. To avoid the singularity in the transformation from the body coordinates to the fixed coordinates, Evans (1977) defined the quaternion parameters:

$$\begin{cases}\chi=\cos(\theta/2)\cos((\psi+\phi)/2),\\ \eta=\sin(\theta/2)\cos((\psi-\phi)/2),\\ \xi=\sin(\theta/2)\sin((\psi-\phi)/2),\\ \zeta=\cos(\theta/2)\sin((\psi+\phi)/2),\end{cases} \tag{14}$$

where θ, ϕ, ψ are the Euler angles to describe the particle orientation. The relation between the quaternion parameters and the angle velocities is

$$\begin{pmatrix}\dot{\xi}\\ \dot{\eta}\\ \dot{\zeta}\\ \dot{\chi}\end{pmatrix}=\frac{1}{2}\begin{pmatrix}-\zeta & -\chi & \eta & \xi\\ \chi & -\zeta & -\xi & \eta\\ \xi & \eta & \chi & \zeta\\ -\eta & \xi & -\zeta & \chi\end{pmatrix}\begin{pmatrix}\Omega_x\\ \Omega_y\\ \Omega_z\\ 0\end{pmatrix}. \tag{15}$$

With the combination of Eqs.(12) and (13), the 3D rotation of a particle can be solved.

COLLISION MODEL

Collision between particles

Particles frequently collide with each other in the high concentrated regime. As shown in Fig.2, the collision of two cylindrical particles is assumed instantaneous and elastic. The contact point and its normal direction are determined by the relative position of two particles. After collision, each particle attains an impulse I along the normal direction. The translational and angular velocities of two particles after collision depend on the impulse and are given as:

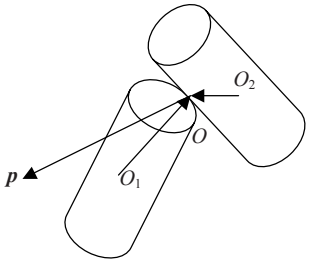

Fig.2 The collision model

$$I\boldsymbol{p} + m_1\boldsymbol{v}_1 = m_1\boldsymbol{v}_1', \tag{16a}$$

$$-I\boldsymbol{p} + m_2\boldsymbol{v}_2 = m_2\boldsymbol{v}_2', \tag{16b}$$

where m and $\boldsymbol{v}$ are the mass and velocity of particle, respectively, $\boldsymbol{p}$ is unit vector along the normal direction, subscripts "1" and "2" are used to distinguish two particles, superscript "′" means after collision. Based on the law of elastic collision, we have

$$k = -(v_{2O}' - v_{1O}')/(v_{2O} - v_{1O}), \tag{17}$$

where k is the elastic coefficient, v_{1O} and v_{2O} are the velocity components of two particles along the normal direction at contact point before collision. The torques exerted on the two particles are $I\boldsymbol{p}\times\boldsymbol{l}_1$ and $-I\boldsymbol{p}\times\boldsymbol{l}_2$, respectively, here $\boldsymbol{l}_1$, $\boldsymbol{l}_2$ are the vectors from mass centre O_1 and O_2 of two particles to the contact point O. Then the rotational equations of particle are

$$\boldsymbol{l}_{1s}\times I\boldsymbol{p}_{1s} + \boldsymbol{J}_1\boldsymbol{\omega}_{1s} = \boldsymbol{J}_1\boldsymbol{\omega}_{1s}', \tag{18a}$$

$$-\boldsymbol{l}_{2s}\times I\boldsymbol{p}_{2s} + \boldsymbol{J}_2\boldsymbol{\omega}_{2s} = \boldsymbol{J}_2\boldsymbol{\omega}_{2s}', \tag{18b}$$

where $\boldsymbol{\omega}$ is the angular velocity of the particle, subscript "s" denotes the body coordinates of particle, $\boldsymbol{J}_1$ and $\boldsymbol{J}_2$ are the rotation inertia moments of the particle. Then the impulse I can be written as

$$\begin{aligned} I = {} & [m_1(1+k)(v_{2O} - v_{1O})]/\{1 + m_1/m_2 \\ & + m_1\{\boldsymbol{A}_1[\boldsymbol{J}_1^{-1}(\boldsymbol{l}_{1s}\times\boldsymbol{p}_{1s})]\}\times\boldsymbol{l}_1\cdot\boldsymbol{p} \\ & + m_1\{\boldsymbol{A}_2[\boldsymbol{J}_2^{-1}(\boldsymbol{l}_{2s}\times\boldsymbol{p}_{2s})]\}\times\boldsymbol{l}_2\cdot\boldsymbol{p}\}, \end{aligned} \tag{19}$$

where $\boldsymbol{A}_1$ and $\boldsymbol{A}_2$ are the transformation matrices which transform the body coordinates to the fixed coordinates (Evans, 1977).

$$\boldsymbol{A} = \begin{pmatrix} -\xi^2+\eta^2-\zeta^2+\chi^2 & -2(\xi\eta+\zeta\chi) & 2(\eta\zeta-\xi\chi) \\ 2(\zeta\chi-\xi\eta) & \xi^2-\eta^2-\zeta^2+\chi^2 & -2(\xi\zeta+\eta\chi) \\ 2(\eta\zeta+\xi\chi) & 2(\eta\chi-\xi\zeta) & -\xi^2-\eta^2+\zeta^2+\chi^2 \end{pmatrix}. \tag{20}$$

Collision with the wall

When particles collide with the wall, the model of collision between particles is also used as long as m_2 is taken as infinite and v_{2O} as 0. Then the transient impulse formula is obtained by reducing Eq.(19):

$$I = m_1(1+k)(-v_{1O})/\{1 + m_1\{\boldsymbol{A}_1[\boldsymbol{J}_1^{-1}(\boldsymbol{l}_{1s}\times\boldsymbol{p}_{1s})]\}\times\boldsymbol{l}_1\cdot\boldsymbol{p}\}. \tag{21}$$

COMPUTATION PARAMETERS

The pipe flow and coordinate system are shown in Fig.3. The pipe diameter and length are 50 mm and 100 mm, respectively. In order to compare the experiment results (Zitoun *et al.*, 2001), all simulations are made at each of two flow rates: 1.577×10^{-4} m^3/s and 3.154×10^{-4} m^3/s, corresponding to Reynolds numbers of 9.4 and 26; and two particle concentrations: 30% and 50%. The particles consist of either cylinders of 8 mm×8 mm, 8 mm×16 mm, 16 mm×16 mm and 16 mm×24 mm (diameter×length) or cubes of 8, 16 and 24 mm, respectively. The lattice spacing is 1 mm. Time step is 1 ms. At inlet and outlet, the periodic boundary condition is used. Initially the fluid has a parabolic velocity profile, the positions and orientations of particles are uniformly distributed, and the particle velocity and angular velocity are zero. It almost takes 24 h to make the statistical average of particle angular velocity and orientation distribution reach a relatively steady state. Following results are given based on the statistical average values.

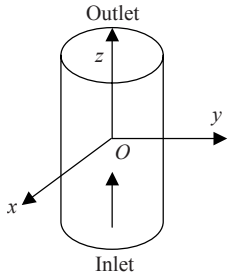

Fig.3 Pipe flow and coordinate system

The computation code and program have been first validated in previous paper (Ku and Lin, 2007), in which the motion and orientation of particles in a suspension of non-Brownian fibers with no inter-particle interactions are studied and compared with the related experiment.

RESULTS AND DISCUSSION

Effect of size and aspect ratios on the angular velocity of particles

The effects of cylindrical particle aspect ratio on

angular velocity about various axes are shown in Fig.4, where the experimental results (Zitoun *et al*., 2001) are also given. Both numerical and experimental results are approximately the same. Rotation about the axial plane (*x* and *y* axes) is greater than that about the radial plane (*z* axis). The increase of particle to pipe size ratio decreases the rotation about all axes because of the increased interactions with other particles and with the wall. Moreover, the increase of particle aspect ratio decreases the rotation because the particles tend to align with the flow directions. Particles with higher aspect ratio have a stronger tendency to align along their length.

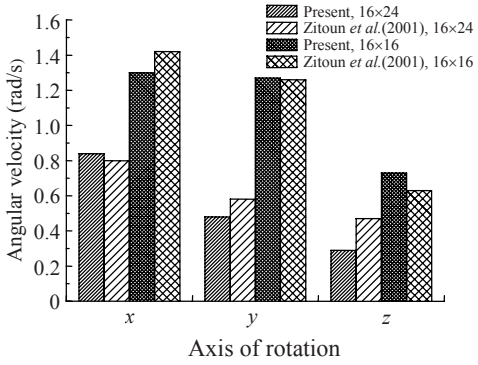

Fig.4 Effect of cylindrical particle aspect ratio on angular velocity about various axes (30% in particle concentration, 26 in Reynolds number)

Effect of cubic particle concentration on the angular velocity of particles

Fig.5 shows the effect of cubic particle concentration on angular velocity about various axes. It can be seen that all rotations of particles decrease with increasing particle concentration from 30% to 50%. It is obvious that increasing particle concentration increases the interaction between particles and decreases the free space available for free motion. The values of angular velocity about three axes are closer for the case of high concentration because the interaction between particles prevents them from rotating.

Effect of Reynolds number on the angular velocity of particles

The effects of Reynolds number on rotation behavior of cubic particles are shown in Fig.6. The flows are still laminar in such region of Reynolds number. Therefore, the torque exerted by fluid on the particles is mainly caused by the average velocity gradient of the fluid. Larger Reynolds number

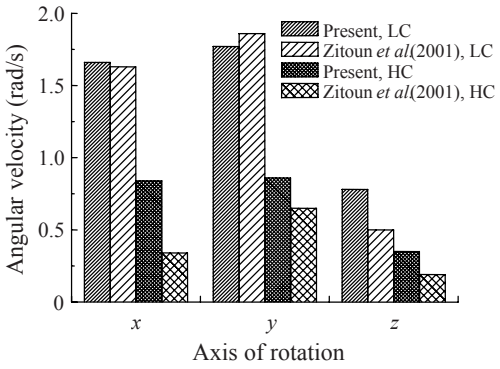

Fig.5 Effect of cubic particle concentration on angular velocity about various axes (9.4 in Reynolds number, 8 mm×8 mm in size, LC: 30% particle concentration; HC: 50% particle concentration)

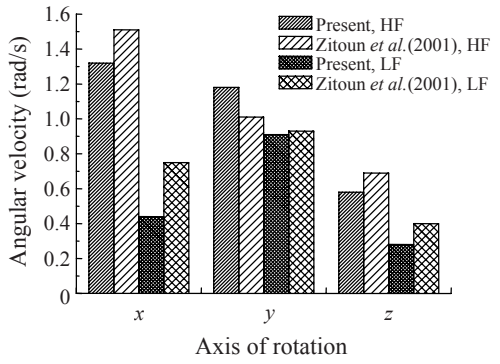

Fig.6 Effect of Reynolds number on angular velocity about various axes (30% in particle concentration, 24 mm×24 mm in size of cubic particles, LF: *Re*=9.4; HF: *Re*=26)

corresponds to larger velocity gradient as well as higher torque which make the particles rotate more drastically.

Effect of particle shape on the angular velocity of particles

The effects of particles shape and size on angular velocity about various axes are plotted in Figs.7a and 7b. We can see that cubic particles rotate faster than cylindrical particles for the same size. Increasing particle size decreases the angular velocity about all axes for the same shape. Compared with cylindrical particles, cubic particles affect the rotation behavior obviously because the cubic particles have many faces and edges, and therefore, a greater chance of interaction with each other and with the wall.

Orientation distribution of cylindrical particles

Figs.8a and 8b show the numerical and

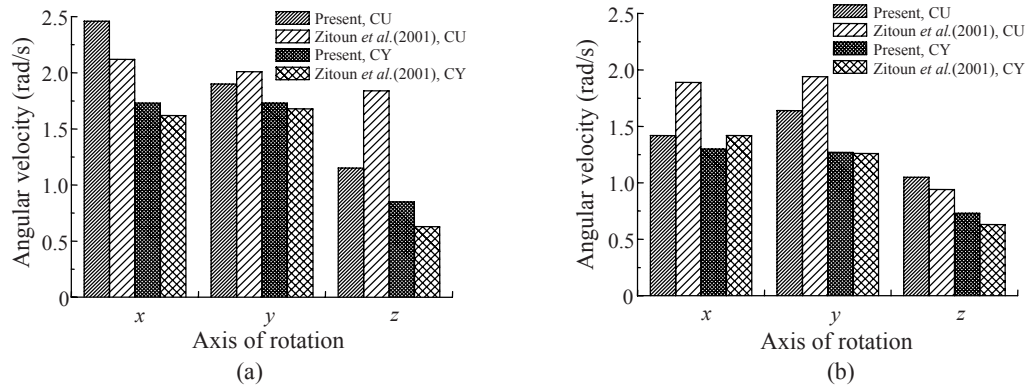

Fig.7 Effect of particle shape on angular velocity about various axes (30% in concentration, 26 in Reynolds number, CU: cubic particles; CY: cylindrical particles). (a) 8 mm×8 mm in size; (b) 16 mm×16 mm in size

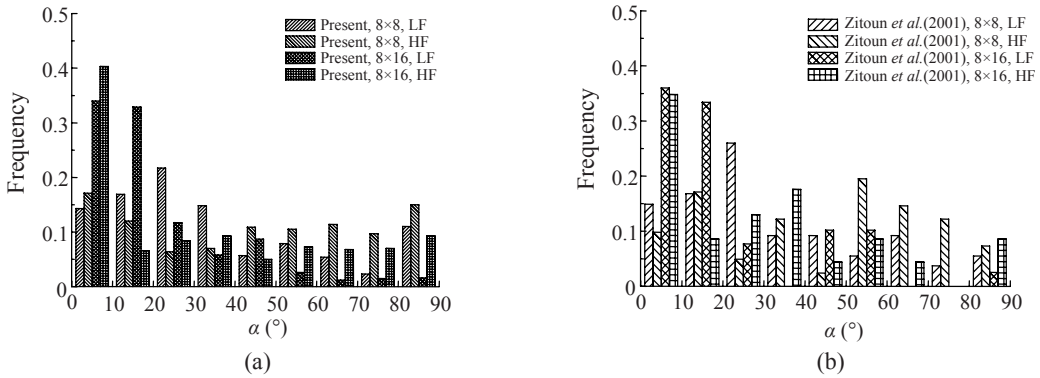

Fig.8 Numerical results (a) and experimental results (b) of orientation distribution for cylindrical particles (30% in concentration, LF: *Re*=9.4; HF: *Re*=26)

experimental results of orientation distribution for cylindrical particles. Abscissa α is the angle of the solid body's major axis with respect to the pipe (z) axis. Both results are in qualitative agreement. From the figures we can see that the higher the aspect ratio is, the more particles orient to the flow direction. This phenomenon is due to the fact that there is a minimum torque exerted on particles when the particles align with the flow direction. This is different from the case with aspect ratio being larger than 5 because, according to the predictions of the Krushkal-Gallily model (Krushkal and Gallily 1988), the orientation is not sensitive to the aspect ratio in that case.

We also can see that more particles have large angles at larger Reynolds number. With decreasing Reynolds numbers, the particles' alignment with the flow direction becomes more obvious.

Orientation distribution of cubic particles

The numerical and experimental results of orientation distribution for cubic particles are plotted in Figs.9a and 9b. Due to the symmetry of a cubic particle, the orientation distributions are only given over the range from 0° to 45°. Compared with the cylindrical particles, the cubic particles have sharp edges, which increase the rotation and even the orientation. It can be seen that the cubic particles show no trend to align with the flow direction, and that the orientations are spread all over the range with no significant difference in magnitude. This phenomenon is due to the symmetry effect of a cubic particle when it rotates. The Reynolds numbers have no obvious effect on the orientations of cubic particles.

Comparison of velocity profile with and without particles

Fig.10 gives the velocity profiles with and without particles at the outlet of pipe when the flow attains a relatively steady state. The velocity profile without particles is a parabola as shown with dash line because the flow is laminar. However, the velocity profile with particles is quite different from the pa-

rabola as shown with solid line. It illustrates that the presence of the particles changes the velocity profile of the carrier fluid due to the large momentum transfer between the two phases.

Function of interactions between particles and between particle and wall

In a dilute particle suspension, the mechanical interaction between particles is insignificant, whereas in the concentrated one the mechanical interaction is dominant. There are some functions of interactions between particles and between particle and wall. Firstly, the interaction causes the frequent motion change of particles due to the changing effect between particles with time. Secondly, the interactions between particles and between particle and wall also have an influence on the mixture of the flow, especially when particle length is of the same order as the pipe dimension. Thirdly, the particles interacting with other particles or wall do not orient to the flow direction as obviously as those particles without interaction. In the latter the hydrodynamic force is dominant.

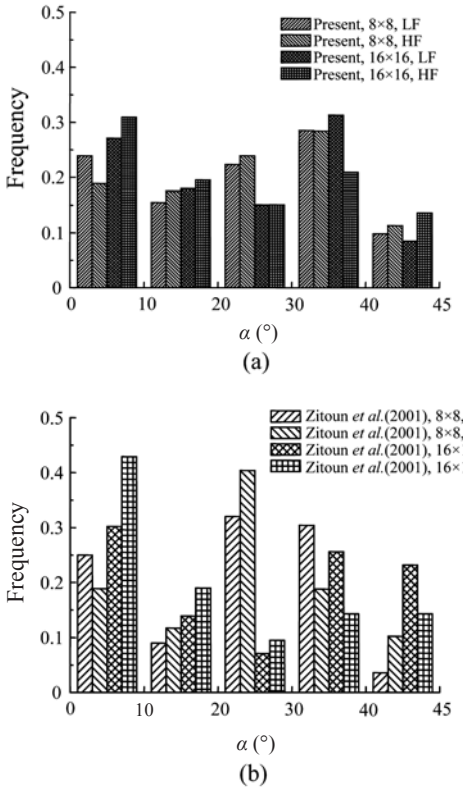

Fig.9 Numerical results (a) and experimental results (b) of orientation distribution for cubic particles (30% in particle concentration, LF: *Re*=9.4; HF: *Re*=26)

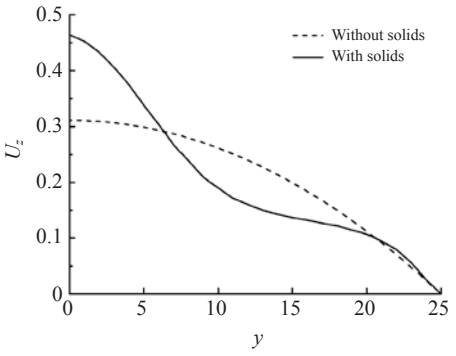

Fig.10 Velocity profiles with and without cylindrical particles at the outlet of pipe (30% in concentration, 26 in Reynolds number, 16 mm×16 mm in size)

CONCLUSION

The angular velocity and orientation distribution of cylindrical and cubic particles in pipe flow with high concentration and high particle to pipe size ratio are simulated numerically using Lattice Boltzmann method. The simulated results are consistent qualitatively with the experimental results available in literature, and show that the rotation of cylindrical particles about the axial plane is greater than that about the radial plane. The increase of cylindrical particle to pipe size ratio decreases the rotation about all axes, and the increase of cylindrical particle aspect ratio decreases the rotation. All rotations of cubic particles decrease with increasing the particle concentration. The angular velocities about three axes are closer for the case of high cubic particle concentration. The cubic particles in the flow with large Reynolds number rotate more drastically. The cubic particles rotate faster than the cylindrical particles for the same size. Increasing particle size decreases the angular velocity about all axes for the same shape. The cylindrical particles with higher aspect ratio tend to align with the flow direction, and the particles' alignment with the flow direction becomes more obvious with decreasing Reynolds numbers. However, the cubic particles show no trend to align with the flow direction, and the orientations are spread all over the range with no significant difference in magnitude. The Reynolds numbers have no obvious effect on the orientations of cubic particles. The presence of the particles changes the velocity profile of the carrier fluid greatly. The interactions between particles and

between particle and wall make the particles not orient to the flow direction as obviously as those particles without interaction do.

References

Ausias, G., Fan, X.J., Tanner, R.I., 2006. Direct simulation for concentrated fibre suspensions in transient and steady state shear flows. *J. Non-Newtonian Fluid Mech*., **135**(1):46-57. [doi:10.1016/j.jnnfm.2005.12.009]

Bernstein, O., Shapiro, M., 1994. Direct determination of the orientation distribution function of cylindrical particles immersed in laminar and turbulent flow. *J. Aerosol. Aci*., **25**(1):113-136. [doi:10.1016/0021-8502(94)90185-6]

Bhatnagar, P.L., Gross, E.P., Krook, M., 1954. A model for collision processes in gases. I: Small amplitude processes in charged and neutral one-component system. *Phys. Rev*., **94**(3):511-525. [doi:10.1103/PhysRev.94.511]

Chen, H., Chen, S., Matthaeus, W.H., 1992. Recovery of the Navier-Stokes equations using a Lattice-gas Boltzmann method. *Phys. Rev*. *A*, **45**(8):R5339-R5342. [doi:10.1103/PhysRevA.45.R5339]

Chen, S., Doolen, G.D., 1998. Lattice Boltzmann method for fluid flows. *Ann. Rev. Fluid Mech.*, **30**(1):329-364. [doi:10.1146/annurev.fluid.30.1.329]

Ding, E., Aidun, C., 2000. The dynamics and scaling law for particles suspended in shear flow with inertia. *J. Fluid Mech.*, **423**:317-344. [doi:10.1017/S0022112000001932]

Evans, D. J., 1977. On the representation of orientation space. *Molecular Physics*, **34**(2):317-325. [doi:10.1080/00268977700101751]

Krushkal, E.M., Gallily, I., 1988. On the orientation distribution function of non-spherical aerosol particles in a general shear flow—II: The turbulent case. *J. Aerosol. Aci*., **19**(2):197-211. [doi:10.1016/0021-8502(88)90223-6]

Ku, X.K, Lin, J.Z, 2007. Orientational distribution of fibres in sheared fibre suspensions. *Chinese Physics Letters*, **24**(6):1622-1625.

Ladd, A.J.C., 1994a. Numerical simulations of particulate suspensions via a discretized Boltzmann equation. Part 1. Theoretical foundation. *J. Fluid Mech.*, **271**:285-309. [doi:10.1017/S0022112094001771]

Ladd, A.J.C., 1994b. Numerical simulations of particulate suspensions via a discretized Boltzmann equation. Part 2. Numerical results. *J. Fluid Mech.*, **271**:311-339. [doi:10.1017/S0022112094001783]

Lin, J.Z., Zhang, W.F., Wang, Y.L., 2002. Research on the orientation distribution of fibers immersed in a pipe flow. *Journal of Zhejiang University SCIENCE*, **3**(5):501-506.

Lin, J.Z., Zhang, W.F., Yu, Z.S., 2004. Numerical research on the orientation distribution of fibers immersed in laminar and turbulent pipe flows. *J. Aerosol. Aci*., **35**(1):63-82.

Qi, D., 2001. Simulations of fluidization of cylindrical multi-particles in a three-dimensional space. *Int. J. Multiphase Flow*, **27**(1):107-118. [doi:10.1016/S0301-9322(00)00008-2]

Yasuda, K., Henmi, S., Mori, N., 2005. Effects of abrupt expansion geometries on flow-induced fiber orientation and concentration distributions in slit channel flows of fiber suspensions. *Polym. Compos.*, **26**(5):660-670.

Zitoun, K.B., Sastry, S.K., Guezennec, Y., 2001. Investigation of three dimensional interstitial velocity, solids motion, and orientation in solid-liquid flow using particle tracking velocimetry. *Int. J. Multiphase Flow*, **27**(8):1397-1414. [doi:10.1016/S0301-9322(01)00011-8]